ELSEVIER

Journal of Molecular Structure 554 (2000) 211–223

Journal of
MOLECULAR
STRUCTURE

www.elsevier.nl/locate/molstruc

Extended structures controlled by intramolecular and intermolecular hydrogen bonding: a case study with pyridine-2,6-dicarboxamide, 1,3-benzenedicarboxamide and *N*,*N*′-dimethyl-2,6-pyridinedicarboxamide

D.S. Marlin[a], M.M. Olmstead[b], P.K. Mascharak[a,*]

[a]*Department of Chemistry and Biochemistry, University of California, Santa Cruz, Santa Cruz, CA 95064, USA*
[b]*Department of Chemistry, University of California, Davis, Davis, CA 95616, USA*

Received 14 February 2000; accepted 24 May 2000

Abstract

The small organic molecule pyridine-2,6-dicarboxamide, although known in the literature for some time, exhibits interesting and previously unexplored intermolecular and intramolecular hydrogen bonding both in solid state and in solution. With the aid of X-ray crystallography and variable-temperature NMR spectroscopy, we here demonstrate the presence of a very strong hydrogen bonding network for this molecule both in condensed state and solution. Furthermore, a novel extended hydrogen bonding graph-set has been derived for this molecule in crystalline state. Comparison of pyridine-2,6-dicarboxamide with 1,3-benzenedicarboxamide, where the intramolecular hydrogen bonding to the pyridine ring in the former has been removed, yields a different intermolecular hydrogen bonded structure in the solid state. A new graph-set has been determined for the extended structure of 1,3-benzenedicarboxamide in the solid state. In solution, 1,3-benzenedicarboxamide is shown to maintain a hydrogen bonding pattern that is weaker than that observed with pyridine-2,6-dicarboxamide. Replacement of one hydrogen on each carboxamide nitrogen of pyridine-2,6-dicarboxamide by a methyl group also alters the extended structure to a significant extent. In *N*,*N*′-dimethyl-2,6-pyridinedicarboxamide, the three-dimensional hydrogen bonding pattern observed with pyridine-2,6-dicarboxamide all but collapses to one-dimensional chains.

Keywords: Hydrogen bonding; Graph-sets; Pyridine-2,6-dicarboxamide; *N*,*N*′-dimethyl-2,6-pyridinedicarboxamide; 1,3-benzenedicarboxamide

1. Introduction

One does not need to look far into the chemical literature to note the intense interest that interactions between molecules, in particular hydrogen bonds, have generated [1–22]. Indeed, there has been an enormous effort in recent years to control hydrogen bond formation [2–6]. The hydrogen bond is one of the most effective and common forces by which self-assembly and self-organization can be achieved to form discrete assemblies and extended lattices both in solid state and in solution [2–6] Hydrogen bonding in liquids governs the formation of liquid crystals, molecular layers, films, mesophases, as well as molecular

0022-2860/00/$ - see front matter
PII: S0022-2860(00)00673-6

recognition [2–7]. In solid state, crystalline architectures built upon hydrogen bonding networks are finding utility in crystal engineering and new materials [7–10]. Hydrogen bonding interactions, especially those of amides, are also important in medicinal chemistry. In one avenue of this field, molecules with specific hydrogen bond donors and acceptors are being used to interact with DNA in desired ways [11–15].

A graph-set formalism has been established to understand and communicate findings in the area of intermolecular hydrogen bonding [16–22]. Rules for assigning graph-sets to particular networks of hydrogen bonds in organic crystals have been described elsewhere [16,22] Attempts have also been made to use graph-sets in predicting hydrogen bonding patterns in solid state structures of small organic molecules with multiple hydrogen bond donors and acceptors [22]. In recent years, reports on the mathematical foundation for such pursuit and the necessary software developments have appeared [23].

In our effort to synthesize designed ligands with carboxamide nitrogens as donors, we recognized the high propensity of pyridine-2,6-dicarboxamide to form very stable hydrogen bonding networks both in solid state and in solution. The robust hydrogen bonding pattern and the associated graph-set for the extended structure of this compound are unusual. In order to determine the factors that give rise to such structures, we have also looked into the structures of 1,3-benzenedicarboxamide and *N,N′*-dimethyl-2,6-pyridinedicarboxamide. The former compound was selected to determine the effect of intramolecular hydrogen bonding on the overall structure. This benzene derivative forms an interesting extended solid state structure governed by intermolecular hydrogen bonds. *N,N′*-dimethyl-2,6-pyridinedicarboxamide was studied to elucidate what changes in the extended structure occur when the extent of intermolecular hydrogen bonding is reduced. Here we report the extended structures of all three compounds in the solid state, the hydrogen bonding patterns associated with these structures, and the results of variable-temperature NMR studies for pyridine-2,6-dicarboxamide and 1,3-benzenedicarboxamide.

2. Experimental section

Pyridine-2,6-dicarboxylic acid, methylamine (2.0 M in THF), isophthaloyl dichloride, and thionyl chloride were purchased from Aldrich Chemical Co. and were used without further purification. Ethanol was distilled from magnesium ethoxide and THF was distilled from sodium and benzophenone prior to use. Pyridine-2,6-dicarboxamide was prepared according to a published procedure [24].

N,N′-dimethyl-2,6-pyridinedicarboxamide: A batch of 3 g (18 mmol) of pyridine-2,6-dicarboxylic acid was added to 10 ml of thionyl chloride and heated to reflux until completely dissolved. The volatiles were then removed under vacuum and the residue was triturated twice with THF. The remaining solid was then dissolved in 30 ml of THF and added dropwise to a solution of methylamine (15.0 ml of 2.0 M THF solution) in THF (50 ml) at 0°C. After the addition was complete, the mixture was warmed to room temperature and stirred for 5 h. The precipitate that formed during this step was removed by filtration, and redissolved in 40 ml of water. This aqueous solution was then made basic with K_2CO_3 and extracted with methylene chloride (3×30 ml). The extracts were combined, dried over $MgSO_4$ and the solvent was finally removed by rotary evaporation. The residue was recrystallized from methylene chloride (overall yield: 2.0 g, 64%). ^{1}H NMR (500 MHz, [D_6]DMSO, 25°C, TMS), δ(ppm) = 2.89 (d, 6H), 8.15 (m, 3H), 9.27 (q, 2H). Selected IR bands (KBr pellet, cm^{-1}): 3323 (s, ν_{NH}), 3294 (s, ν_{NH}), 1687 (s, ν_{CO}), 1659 (s, ν_{CO}), 1543 (s), 1443 (vs), 1401 (s), 1243 (m) 1165 (m), 740 (m), 681 (s), 645 (m).

1,3-Benzenedicarboxamide: A batch of 2 g (9.9 mmol) of isophthaloyl dichloride was dissolved in 10 ml of ethanol and warmed to 60°C for 2 h. The volatiles were then removed in vacuum and the residue was taken up in10 ml of water. This solution was cooled to 0°C and to this was slowly added a solution of aqueous ammonium hydroxide (40 ml). The mixture was heated to 100°C for 2 h and then allowed to cool to room temperature and filtered. The precipitate was washed twice with water (10 ml) and dried under vacuum. The white solid was recrystallized from water (overall yield: 1.3 g, 80%). ^{1}H NMR (500 MHz, [D_6]DMSO, 25°C, TMS), δ(ppm) = 7.46 (s, 2H), 7.53 (t, 1H), 8.00 (d,

Table 1
Crystallographic data for pyridine-2,6-dicarboxamide (prisms), 1,3-benzenedicarboxamide and *N*,*N*′-dimethyl-2,6-pyridinedicarboxamide

	Pyridine-2,6-dicarboxamide	1,3-benzene-dicarboxamide	*NN*′-dimethyl-2,6-pyridinedicarboxamide
Empirical formula	$C_7H_7N_3O_2$	$C_8H_8N_2O_2$	$C_9H_{11}N_3O_2$
Crystal habit	prism	block	plate
M_r	165.16	164.16	193.21
Crystal system	monoclinic	monoclinic	orthorhombic
Space group	*C*2/*c*	*C*2/*c*	*Pbca*
a(Å)	12.3963(9)	7.0231(10)	12.4186(8)
b(Å)	7.6380(6)	7.1749(12)	9.8810(7)
c(Å)	8.6729(6)	14.7014(19)	15.7409(10)
α (°)	90	90	90
β (°)	120.2800(10)	93.927(11)	90
γ (°)	90	90	90
V(Å^3)	709.14(9)	739.06(19)	1931.5(2)
T (K)	90(2)	133(2)	90(2)
Z	4	4	8
Crystal size (mm)	$0.36 \times 0.20 \times 0.16$	$0.10 \times 0.10 \times 0.10$	$0.37 \times 0.13 \times 0.04$
ρ_{calcd} (g cm^{-3})	1.547	1.475	1.329
Radiation λ (Å)	0.71073	1.54178	0.71073
μ (mm^{-3})	0.118	0.908	0.097
Max. and min. transm.	0.9814 and 0.9589	0.9146 and 0.9146	0.9961 and 0.9650
R_1[a] (obs'd data)	0.0460	0.0309	0.0448
$wR2$[b] (all data)	0.1339	0.0841	0.1016

[a] $R_1 = \sum \|F_o - F_c\| / \sum |F_o|$.
[b] $wR_2 = (\sum(w(F_o^2 - F_c^2)^2) / \sum(w(F_o^2)^2))^{1/2}$.

2H), 8.04 (s, 2H), 8.38 (s, 1H). Selected IR bands (KBr pellet, cm^{-1}): 3367 (s, ν_{NH}), 3155 (s, ν_{NH}), 1659 (s, ν_{CO}), 1627 (s), 1575 (m), 1395 (s), 1128 (s), 797 (m), 643 (s), 620 (m).

Instrumentation: A Perkin–Elmer 1600 FTIR spectrophotometer was employed to monitor the IR spectra and the ^{1}H NMR spectra were monitored on a Varian 500 MHz Unity Plus instrument interfaced with a Sun OS 4.1.3 computer.

X-ray structure determination: Needles of pyridine-2,6-dicarboxamide were grown from a saturated solution of H_2O or by layering H_2O on a DMSO solution of the compound and allowing for slow diffusion at room temperature. Prisms of this compound were grown by slow cooling of saturated solutions of this compound in ethanol, pyridine, or nitromethane. The crystal used for X-ray data collection was grown from pyridine. Large colorless blocks of 1,3-benzenedicarboxamide were grown from H_2O. In case of *N*,*N*′-dimethyl-2,6-pyridinedicarboxamide, colorless plates were grown from slow evaporation of a solution of the compound in methylene chloride. X-ray data for *N*,*N*′-dimethyl-2,6-pyridinedicarboxamide and the prisms of pyridine-2,6-dicarboxamide were collected on a Bruker SMART 1000 system with the use of MoKα radiation. The low temperature N_2 stream was generated by a CryoIndustries apparatus. No decay in the intensities from 50 remeasured frames was detected. For 1,3-benzenedicarboxamide, data were obtained on a Siemens P4 diffractometer equipped with a Siemens rotating copper anode, nickel filter, and LT-2 low temperature device. A linear scale to the intensities was applied to accomodate a 3.4% decay in the intensities of two standard reflections. All structures were solved by direct methods (SHELXS-97) and refined using all data, based on F^2 (SHELXL-97). No absorption corrections were applied. Hydrogen atoms were located on difference maps and freely refined.

Crystal data and data collection parameters are summarized in Table 1, while selected bond distances are included in Fig. 1. A list of hydrogen bond

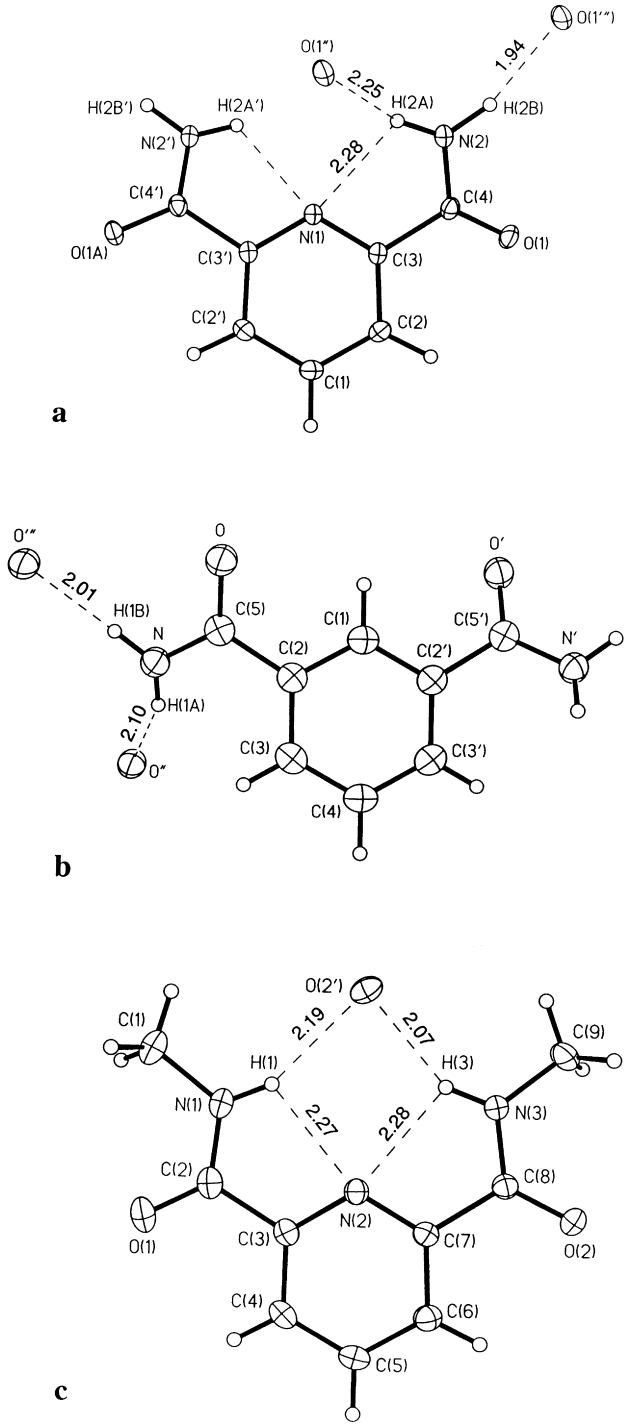

Fig. 1. Drawings of pyridine-2,6-dicarboxamide (structure a), 1,3-benzenedicarboxamide (structure b), and *N*,*N*′-dimethyl-2,6-pyridinedicarboxamide (structure c) showing the unique set of hydrogen bonds, the atom numbering scheme, and thermal elliposids at the 50% probability level. Selected hydrogen bond distances (Å) are shown. In structure a, intermolecular hydrogen bonds originating from N(2′) are omitted for clarity. Similarly, intermolecular hydrogen bonds originating from O, O′ and N′ are omitted in structure b.

Table 2
Hydrogen bonding distances and angles for pyridine-2,6-dicarboxamide, 1,3-benzenedicarboxamide and *N*,*N*′-dimethyl-2,6-pyridinedicarboxamide. The hydrogen bond donor atoms are denoted as D and the acceptors as A

D–H···A[a]	*d*(D–H) (Å)	*d*(H···A) (Å)	*d*(D···A) (Å)	DHA (°)
Pyridine-2,6-dicarboxamide				
N(2)–H(2A)···O(1″)#2	0.917(15)	2.251(15)	3.0691(11)	148.3(14)
N(2)–H(2B)···O(1‴)#3	0.967(16)	1.940(17)	2.8653(11)	159.4(13)
1,3-benzenedicarboxamide				
N–H(1A)···O″#2	0.889(18)	2.096(19)	2.9035(17)	150.4(15)
N–H(1B)···O‴#3	0.89(2)	2.01(2)	2.8998(18)	173.7(18)
N,*N*′-dimethyl-2,6-pyridinedicarboxamide				
N(1)–H(1)···O(2′)#1	0.894(16)	2.193(17)	3.0302(16)	155.7(14)
N(3)–H(3)···O(2′)#1	0.901(17)	2.071(18)	2.8802(15)	149.0(14)

[a] Symmetry transformations used to generate equivalent atoms: #1, $-x$, y, $-z + 1/2$; #2, $x + 1/2$, $y - 1/2$, z; and #3, $-x + 1/2$, $-y + 1/2$, $-$z.

distances and angles is provided in Table 2. The rest of the crystallographic data has been submitted as supplementary material.

3. Results and discussion

Pyridine-2,6-dicarboxamide can be readily recrystallized (within minutes) from several solvents and depending on the type of solvent used, it affords either prisms or needles. Needles were grown from H_2O or DMSO/H_2O, while prisms were obtained by recrystallization from pyridine, ethanol, or nitromethane. The structure of pyridine-2,6-dicarboxamide was determined for both the needle and the prism morphologies and it was found to be the same. The crystal data for the prismatic form are listed in Table 1. X-ray quality blocks of 1,3-benzenedicarboxamide were grown from H_2O and were also obtained rapidly (within less than an hour). *N*,*N*′-dimethyl-2,6-pyridinedicarboxamide is much more soluble than pyridine-2,6-dicarboxamide and readily dissolves in alcohols, water, THF, methylene chloride and acetonitrile. Crystallization of this compound was achieved by slow evaporation of its solution in methylene chloride or ethanol. Plates were obtained from both solvents. It is interesting to note that although strongly hydrogen bonding solvents such as H_2O, DMSO and ethanol were used to recrystalize the above compounds, in no case did the solvent form part of the crystal structure.

Views of pyridine-2,6-dicarboxamide (Fig. 1a), 1,3-benzenedicarboxamide (Fig. 1b), and *N*,*N*′-dimethyl-2,6-pyridinedicarboxamide (Fig. 1c) with relevant hydrogen bonding distances and numbering scheme are shown in Fig. 1.[1]. Hydrogen bonding distances and angles are summarized in Table 2. In Fig. 1 and Table 2, the D–H bonds have not been extended to the typical neutron diffraction value of 1.020 Å, a practice often followed in rigorous crystallographic studies [25]. Each molecule has 2-fold symmetry that passes through N(1) and C(1) in pyridine-2,6-dicarboxamide, C(1) and C(4) in 1,3-benzenedicarboxamide, and N(2) and C(5) in *N*,*N*′-dimethyl-2,6-pyridinedicarboxamide (the 2-fold symmetry is non-crystallographic in this case). The crystal structure of pyridine-2,6-dicarboxamide reveals that there are two long N–H···N intramolecular hydrogen bonds per molecule between the pyridyl nitrogen N(1) and the carboxamide hydrogens H(2A) and H(2A′) on either side of it (Fig. 1a). The two intermolecular hydrogen bonds between (i) N(2) and O(1″) and (ii) N(2) and O(1‴) form half of an eight membered hydrogen bonding ring between four individual molecules. This type of hydrogen bonding motif in which an eight membered hydrogen bonding ring forms between four individual molecules is called an $R_4^2(8)$ set in graph-set nomenclature. In this nomenclature, $R_4^2(8)$ describes a hydrogen bonding pattern where R represents a ring, the

[1] In two of the three molecules, the asymmetric unit is smaller than one molecule due to point symmetry and hence the IUPAC numbering scheme cannot be easily applied. For this reason, the numbering scheme in Fig. 1 assigns atom numbers in a consecutive fashion to the atoms of the asymmetric unit.

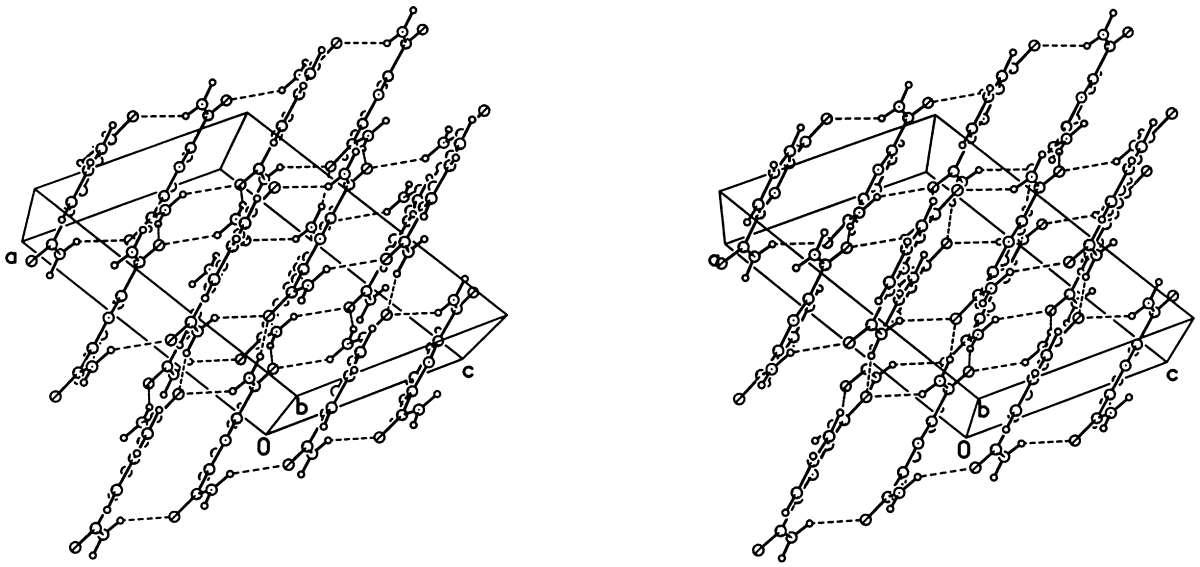

Fig. 2. A stereo view of pyridine-2,6-dicarboxamide that reveals the honeycomb-like pattern created by the $R_4^2(8)$ graph-sets. Intramolecular hydrogen bonds omitted for clarity.

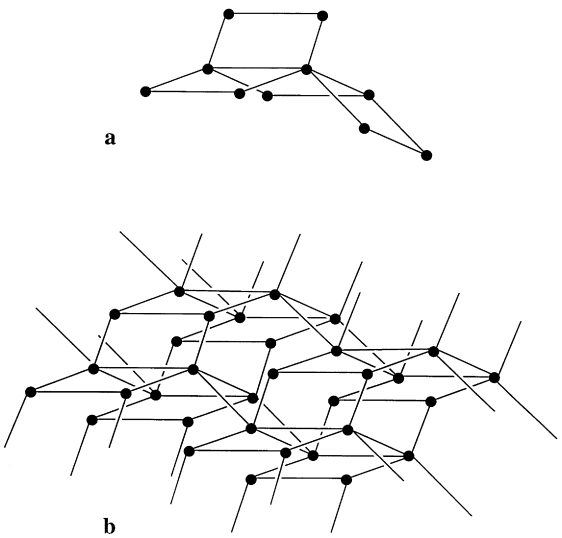

Fig. 3. (a) A graph-set drawing for pyridine-2,6-dicarboxamide. Individual molecules are represented as dots and intermolecular hydrogen bonds are shown as lines. (b) The graph-set in three dimensions (vertical extension of the structure is omitted at several points for clarity).

superscript and subscript are the number of hydrogen bond acceptors and donors, respectively, and the number in brackets refers to how many members make up the ring [16]. The $R_4^2(8)$ graph-set pattern is the basis of the extended structure for pyridine-2,6-dicarboxamide. The amido groups are not in the pyridyl plane, and this is what leads to the propagation of the $R_4^2(8)$ hydrogen bonded rings in two directions (Fig. 2). The propagation directions can be related to the direction of the C(4)–O(1) lines. Within one molecule, the dihedral angle between C(4)–O(1) and C(4′)–O(1′) is 132.4°. Also, the C(4)–O(1) line is tipped 15.4° above the pyridyl plane while C(4′)–O(1′) is tipped −15.4° below it. The planes formed by the repeating $R_4^2(8)$ sets give rise to a honeycomb-like three-dimensional structure as shown in Fig. 2. In this stereo view diagram, the repeating $R_4^2(8)$ sets that form planes propagating in two directions are clearly visible.

Using the graph-set formalism and representing the individual molecules as dots and the intermolecular hydrogen bonding between these molecules as lines, the hydrogen bonding network around a central molecule can be simplified to the one shown in Fig. 3a. An extension of the simplified drawing of Fig. 3a is shown in Fig. 3b. In the simplified version, the

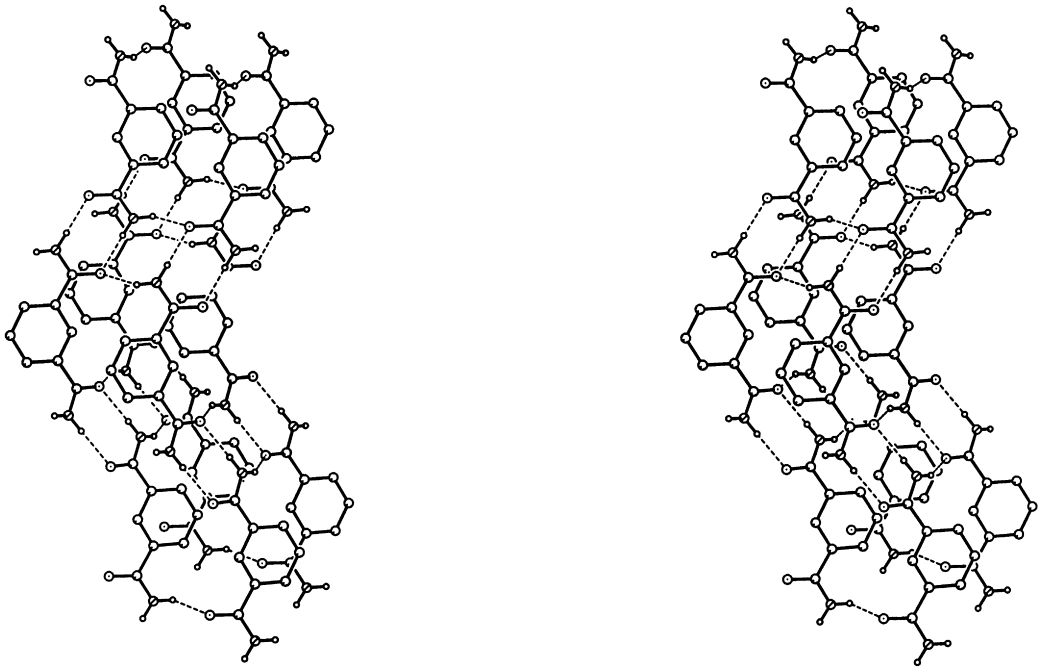

Fig. 4. Stereo view of 1,3-benzenedicarboxamide showing a segment of the up/down–up/down $R_2^2(8)/R_4^2(8)$ staircase-like motif.

$R_4^2(8)$ graph-sets can be clearly seen as four membered rings arranged in a crinkled sheet-like fashion in two directions. Each molecule sits at an intersection between these sheets (Fig. 3b). It is also apparent that from each molecule, four $R_4^2(8)$ graph-sets are generated, three of these $R_4^2(8)$ sets share a common molecule (in addition to the one from which they stem) which gives rise to a paddle-wheel type motif with three blades. The fourth $R_4^2(8)$ set connects this paddle-wheel to two adjacent sheets (Fig. 3b). To the best of our knowledge, this robust and elegant three-dimensional array of $R_4^2(8)$ hydrogen bonding motifs has not been shown or predicted yet for any other hydrogen bonded lattice.

Replacement of the pyridine ring of pyridine-2,6-dicarboxamide with the benzene ring in 1,3-benzenedicarboxamide (Fig. 1b) removes the intramolecular hydrogen bonding. As a result of this alteration, the amide hydrogens are not held in place and rotate. In the solid state, the two amide groups are furthest apart from each other (Fig. 1b). This has a profound effect on the intermolecular hydrogen bonding scheme as shown in Fig. 4. The extended structure for this molecule comprises alternating $R_4^2(8)$ and $R_2^2(8)$ graph-set motifs. This type of alternating $R_4^2(8)/R_2^2(8)$ motif has been demonstrated for other terminal amides [16]. A stereo view of this molecule showing the three-dimensional propagation of the $R_4^2(8)$ and $R_2^2(8)$ sheets relative to each other is shown in Fig. 4. The propagation of the sheets in two directions for this molecule arises from the angle of the two NH_2 planes, which are tilted 61.2° with respect to each other. Each molecule sits at the intersection of two sheets. This pattern is more clearly demonstrated when the individual 1,3-benzenedicarboxamide molecules are shown as dots and the hydrogen bonds as lines, as shown in the simplified graph-set pattern of Fig. 5a. Here the $R_2^2(8)$ graph-sets are depicted as bowed lines between two molecules (dots) and the $R_4^2(8)$ sets as four molecule rings with straight lines connecting the two sets of bowed lines together. The 61° angle between the two planes is indicated. The way four such planes interact with each other is depicted in Fig. 5b. In this drawing, it is important to note that the repeating $R_2^2(8)/R_4^2(8)$ sets are not coplanar but form staircase-like patterns that connect each other in an up/down–up/down fashion (Fig. 4). Extension of the simplified graph-set (Fig. 5b) in three dimensions yields a complex network,

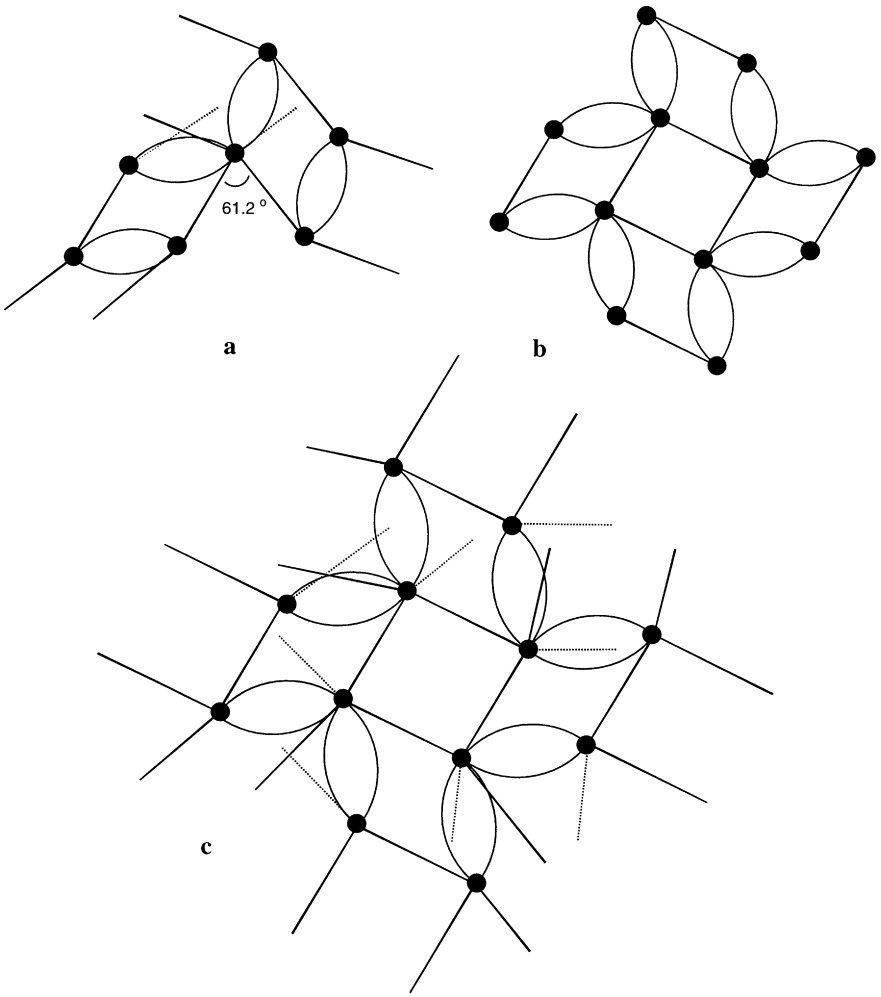

Fig. 5. (a) Graph-set representation of 1,3-benzenedicarboxamide indicating the sheets formed from the repeating $R_2^2(8)/R_4^2(8)$ sets and the angle between them. (b) Four repeating $R_2^2(8)/R_4^2(8)$ sheets are connected to each other in an up/down–up/down fashion. (c) Extension of the graph-set. Selected hydrogen bonds around molecules at the perimeter are omitted for clarity.

which is shown in Fig. 5c. Eight hydrogen bonds originate from each molecule as shown for the central molecules in Fig. 5c. Comparison of Fig. 3b and 5c demonstrates that the presence or absence of intramolecular hydrogen bonding plays a crucial role in formation of the three-dimensional structures of these two similar primary carboxamides, pyridine-2,6-dicarboxamide and 1,3-benzenedicarboxamide.

The crystal structure of *N*,*N*′-dimethyl-2,6-pyridinedicarboxamide is markedly different from that of pyridine-2,6-dicarboxamide and 1,3-benzenedicarboxamide with regard to its extended hydrogen bonding network. Although in the structures of all three compounds a carbonyl oxygen is hydrogen bonded to two NH hydrogens at one time, in the case of the primary amides, the carbonyl oxygen accepts one NH hydrogen from each of two individual molecules (Fig. 1a,b), while in the secondary amide, the carbonyl oxygen O(2′) is bonded to both NH hydrogens (H(1) and H(3)) from the same molecule (Fig. 1c). There are also two long intramolecular hydrogen bonds between the amide NHs (H(1) and H(3)) and the pyridyl nitrogen N(2) in *N*,*N*′-dimethyl-2,6-pyridinedicarboxamide, which gives

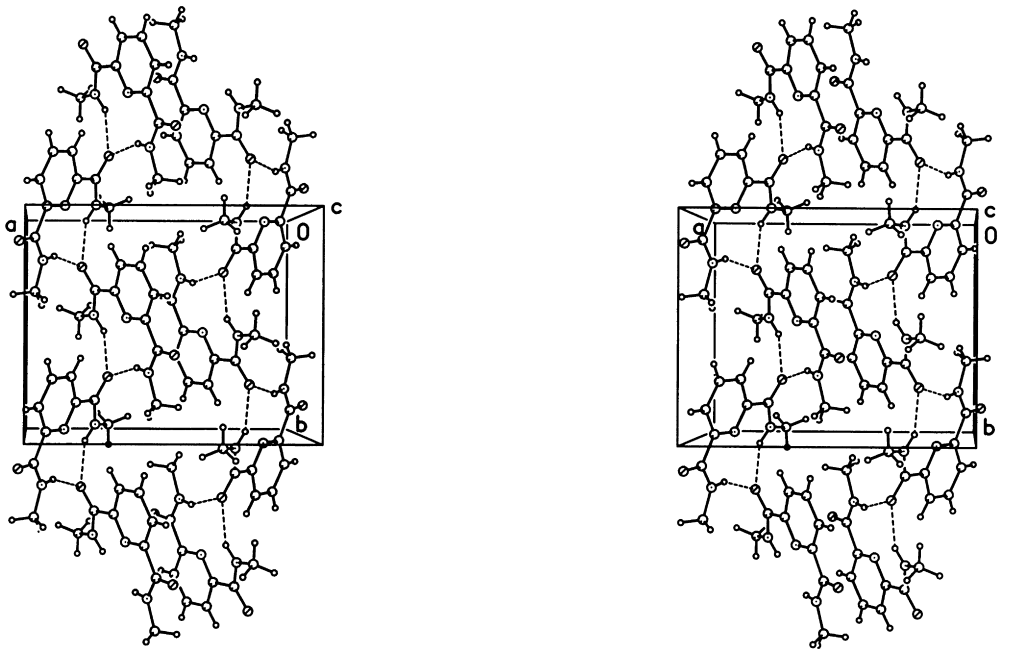

Fig. 6. Stereo view of *N*,*N*′-dimethyl-2,6-pyridinedicarboxamide showing the one-dimensional chains and their packing arrangement in the crystal lattice. Intramolecular hydrogen bonds omitted for clarity.

rise to an internal diamond-like hydrogen bonding network (Fig. 1c). These features allow for propagation of the extended structure in only one dimension as shown in the stereo view of the extended structure for *N*,*N*′-dimethyl -2,6-pyridinedicarboxamide (Fig. 6). From this perspective, the extension of the one-dimensional chains throughout the lattice is demonstrated as well as the way these chains interact with one another.

Secondary carboxamides can have either a *cis* or a *trans* geometry, which refers to the orientation of the alkyl group on the nitrogen relative to the substituent on the carbonyl carbon. In *N*,*N*′-dimethyl-2,6-pyridinedicarboxamide, the two carboxamide groups exist in *trans* configuration most likely due to the intramolecular hydrogen bonding just described (Fig. 1c). The proximity of the two *trans*amide NH donors is the key factor that lends to the one-dimensional structure (Fig. 6) and such mode of hydrogen bonding of one carbonyl oxygen from one molecule to two amide hydrogens of the next molecule is quite unusual [16].

The *trans* amide hydrogen bonding motifs are especially important in biological systems that form the common secondary structures of α-helices and β-sheets, and also in synthetic fibers [8]. Hydrogen bonding in *cis* secondary amides usually results in cyclic dimers ($R_2^2(8)$) or chains in which one carbonyl oxygen accepts only one NH hydrogen (C(4)), where C in the graph-set nomenclature refers to a chain [8]. In the chain motif, a helical two-fold screw axis results due to the formation of a more preferable C=O···H angle (this is also the case for *trans* amide C(4) chains). The preference for the formation of these secondary structures such as helices in the *cis* and *trans* amide chains results from a preferred hybridization angle of hydrogen bonding on the carbonyl oxygen. Taylor et al. have examined the geometries for intermolecular N–H···O=C hydrogen bonds of a large number of compounds contained in the Cambridge Structural Database [26,27]. They concluded that on average, the carbonyl oxygens that accept either one or two NH hydrogens form hydrogen bonds in the direction of the oxygen sp^2 lone pairs with an angle Φ of approximately 130°. All three compounds presented in this report are of the type where the carbonyl oxygen accepts two NH hydrogens. For pyridine-2,6-dicarboxamide, the Φ(angles (are 126(4)° and 140(4)° and

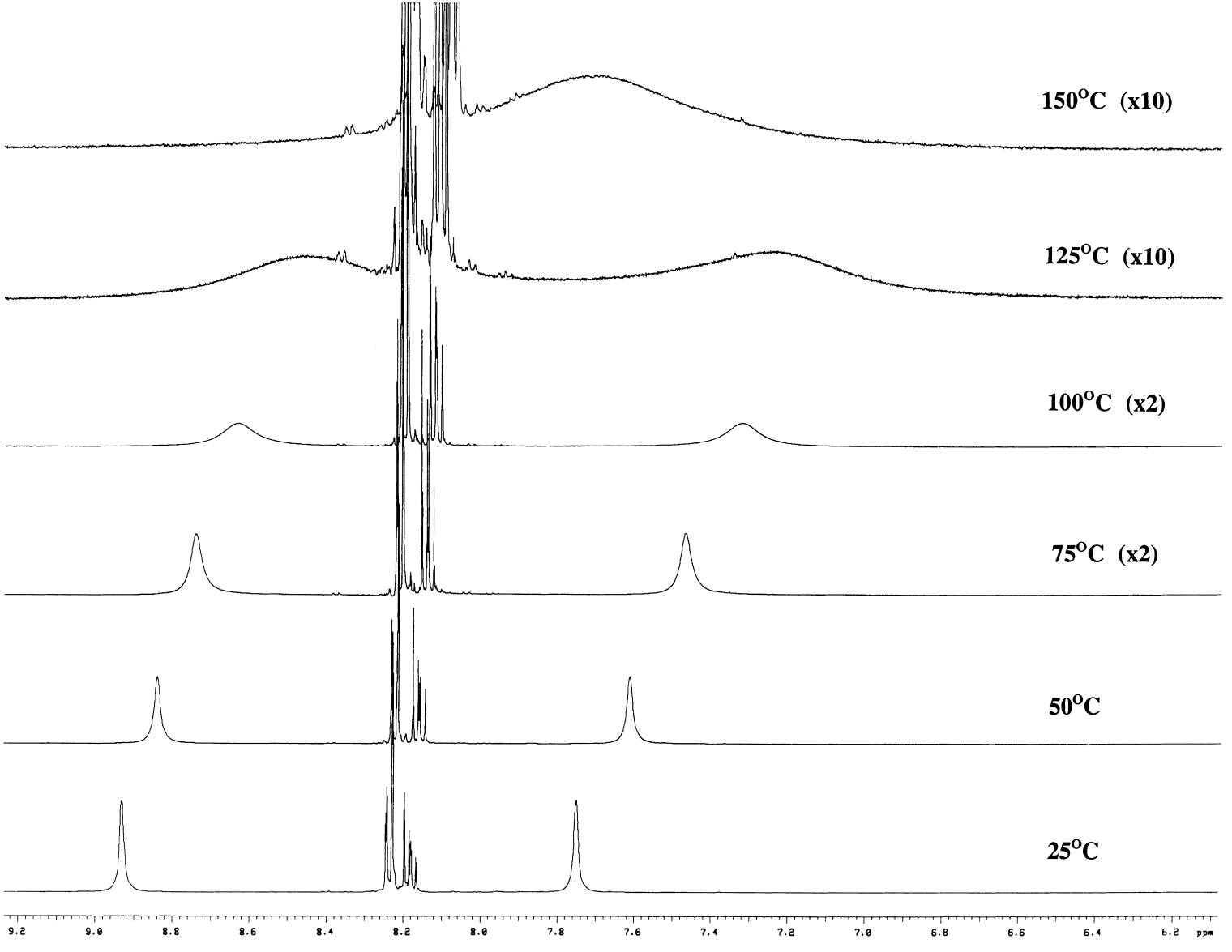

Fig. 7. Variable-temperature ^{1}H NMR spectra of pyridine-2,6-dicarboxamide in $[D_6]$DMSO. Temperature and magnification are indicated for each spectrum.

for 1,3-benzenedicarboxamide, the values are 118(5)° and 144(5)°. It is evident that while pyridine-2,6-dicarboxamide exhibits Φ values in the normal range for primary amides, [26,27] a larger deviation from 130° is noted for 1,3-benzenedicarboxamide. In the case of *N*,*N*′-dimethyl-2,6-pyridinedicarboxamide, a secondary amide, the Φ angles are 104(4)° and 144(4)°. The relatively large deviation from 130° in this case is likely due to the strain arising from the fact that both NH hydrogen donors come from the same molecule (Fig. 1c). It is interesting to note that the extent of hydrogen bonding in the three compounds is diminished (Figs. 2, 4, and 6) as the angle Φ deviates further from 130°.

Infrared (IR) spectroscopy provides additional information for studying hydrogen bonds in the solid state. In the present study, the IR spectra of all three compounds have been examined in KBr matrix. The ν_{CO} for pyridine-2,6-dicarboxamide and 1,3-benzenedicarboxamide appear as a single band at 1670 cm^{-1} and 1659 cm^{-1}, respectively, while for *N*,*N*′-dimethyl-2,6-pyridinedicarboxamide, the carbonyl stretch is split into two peaks with maxima at 1684 cm^{-1} and 1661 cm^{-1}. The reason for this behavior is evident in the crystal structures. In pyridine-2,6-dicarboxamide and 1,3-benzenedicarboxamide, all the carbonyl groups are involved in similar hydrogen bonding (Figs. 2 and 4) while in *N*,*N*′-dimethyl-2,6-pyridinedicarboxamide, only one of two carbonyl groups participates in hydrogen bonding (Fig. 6). The

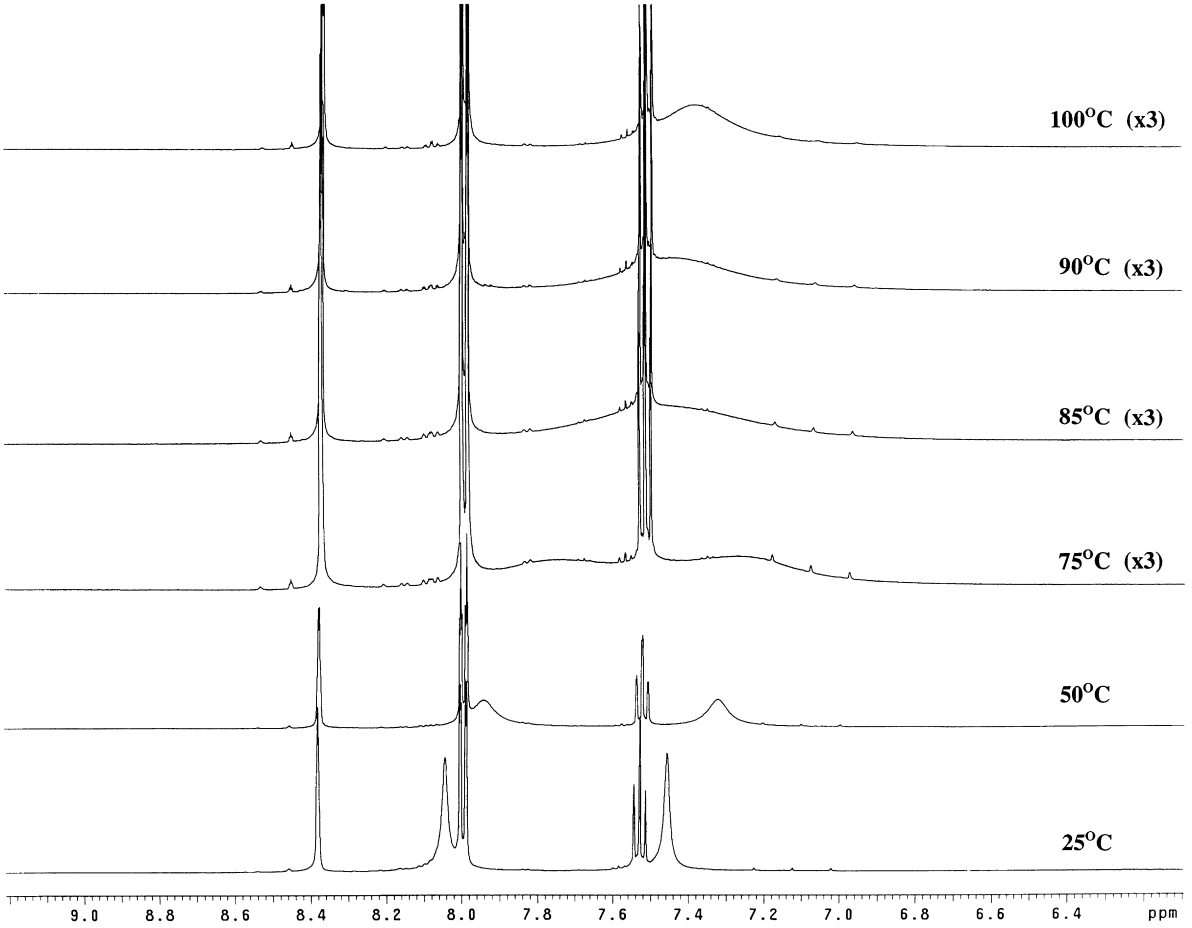

Fig. 8. Variable-temperature ^1H NMR spectra of 1,3-benzenedicarboxamide in [D_6]DMSO. Temperature and magnification are indicated for each spectrum.

NH_2 groups of pyridine-2,6-dicarboxamide and 1,3-benzenedicarboxamide exhibit two ν_{NH} peaks each with maxima at 3406 cm^{-1} and 3231 cm^{-1} for the former, and at 3367 cm^{-1} and 3155 cm^{-1} for the latter. Much smaller splitting (3323 cm^{-1} and 3294 cm^{-1}) is observed in case of *N,N′*-dimethyl-2,6-pyridinedicarboxamide.

With the structures of the title compounds in hand we were curious to find out whether the hydrogen bonding pattern of pyridine-2,6-dicarboxamide and 1,3-benzenedicarboxamide, as noted in solid state, are partially retained in solution. In order to study such bonding in solution, the technique of variable-temperature ^1H NMR spectroscopy was employed for both compounds in [D_6]DMSO. At 25°C in DMSO solution, pyridine-2,6-dicarboxamide exhibits two NH peaks of equal intensity at 8.88 and 7.69 ppm (Fig. 7). Upon warming, the peaks begin to broaden and finally coalesce into one broad peak at ~7.7 ppm at 150°C (Fig. 7). The resistance to disruption of the hydrogen bonding in DMSO solution up to temperatures as high as 150°C implies a very strong hydrogen bonding interaction. From this data, we estimated a rate constant (k_n) of 30.4 s^{-1} and an activation energy ($\Delta G^{\ddagger}$) of 19.0 Kcal/mol for the chemical exchange at the temperature of coalescence using standard procedures [7,28].[2] Similar measurement was also performed on 1,3-benzenedicarboxamide in [D_6]DMSO solution (Fig. 8). At 25°C, this compound also exhibits two sharp peaks of equal intensity for the NH_2 hydrogens at 8.04 and 7.46 ppm (Fig. 8). Upon warming, the NH peaks also coalesce (to a broad peak at ~7.4 ppm) as in the case with pyridine-2,6-dicarboxamide. However, the two peaks for 1,3-benzenedicarboxamide come together at a lower temperature (90°C, Fig. 8). For 1,3-benzenedicarboxamide, k_n and $\Delta G^{\ddagger}$ are 21.4 s^{-1} and 16.7 Kcal/mol, respectively [28]. The 2.3 Kcal/mol difference in activation energy indicates that in solution, the hydrogen bonding interaction of 1,3-benzenedicarboxamide is weaker compared to that of pyridine-2,6-dicarboxamide.

In summary, results of structural and spectroscopic studies on the three amides in solid state clearly demonstrate that the three-dimensional structure of pyridine-2,6-dicarboxamide can be altered to the completely different structure of 1,3-benzenedicarboxamide by removing the intramolecular hydrogen bonds. The same structure collapses to the one-dimensional structure of *N,N′*-dimethyl-2,6-pyridinedicarboxamide upon removal of two intermolecular hydrogen bonds. Although the extended hydrogen bonding motifs seen in crystalline pyridine-2,6-dicarboxamide (Fig. 3) and 1,3-benzenedicarboxamide (Fig. 5) collapse in solution, the NMR data suggest that both compounds maintain substantial hydrogen bonding in DMSO. Further work is required to understand the nature of hydrogen bonding for these molecules in solution.

Acknowledgements

This research was supported by a grant from the National Science Foundation (CHE-9818492). We would like to thank Jim Loo for technical assistance.

References

[1] A.G. Jeffery, W. Saenger, Hydrogen Bonding in Biological Structures, Springer, Berlin, 1991.
[2] J.-M. Lehn, Angew. Chem. Int. Ed. Engl. 29 (1990) 1304.
[3] J.-M. Lehn, Supramolecular Chemistry, VCH, New York, 1995.
[4] Y. Aoyama, in: V. Balzani, L. De Cola (Eds.), Supramolecular Chemistry, Kluwer, Dordrecht, 1992, p. 17.
[5] A.D. Hamilton, in: V. Balzani, L. De Cola (Eds.), Supramolecular Chemistry, Kluwer, Dordrecht, 1992, p. 137.
[6] J.P. Folkers, J.A. Zerkowski, P.E. Laibinis, C.T. Seto, G.M. Whitesides, in: T. Bein (Ed.), Supramolecular Architecture; Synthetic Control in Thin Films and Solids, American Chemical Society, Washington, DC, 1992, p. 10.
[7] M. Suarez, J.-M. Lehn, S.C. Zimmerman, A. Skoulios, B. Heinrich, J. Am. Chem. Soc. 120 (1998) 9526.
[8] J. Bernstein, M.C. Etter, L. Leiserowitz, in: H.B. Burgi, J.D. Dunitz (Eds.), Structure Correlation, 2, VCH, Weinheim, 1993, p. 431.
[9] G.R. Desiraju, Crystal Engineering. The Design of Organic Solids, Elsevier, Amsterdam, 1989.
[10] J. Hulliger, Angew. Chem. Int. Ed. Engl. 33 (1994) 143.
[11] A.K. Todd, A. Adams, J.H. Thorpe, W.A. Denny, L.P.G. Wakelin, C.J. Cardin, J. Med. Chem. 42 (1999) 536.
[12] M.E. Peek, L.A. Lipscomb, J.A. Bertrand, Q. Gao, P. Roques,

[2] The rate constant was calculated by using the equation $k_n = \pi(\partial\nu)/2^{1/2}$, where $(\partial\nu)$ corresponds to the chemical shift difference (in Hz) of the signals exchanging. The energy barrier at the temperature of coalescence was calculated with the equation $(\Delta G^{\ddagger}) = RT_c(22.96 + \ln(T_c/\partial\nu))$ (J/mol), where T_c is the temperature of coalescence (in K).

C. Garbay-Jaureguiberry, L.D. Williams, Biochemistry 33 (1994) 3794.
[13] L.D. Williams, M. Egli, Q. Gao, P. Bash, G.A. van der Marel, J.H. van Boom, A. Rich, J.-H.A. Wang, C.A. Fredrick, Proc. Natl. Acad. Sci. USA 87 (1990) 2225.
[14] P.R. Lowe, C.E. Sansom, C.H. Schwalbe, M.F.G. Stevens, A.S. Clark, J. Med. Chem. 35 (1992) 3377.
[15] H. Li, B.M. Goldstein, J. Med. Chem. 35 (1992) 3560.
[16] M.C. Etter, Acc. Chem. Res. 23 (1990) 120.
[17] M.C. Etter, Isr. J. Chem. 25 (1985) 312.
[18] M.C. Etter, J. Phys. Chem. 95 (1991) 4602.
[19] M.C. Etter, J. Bernstein, J.M. MacDonald, Acta Cryst. B 46 (1990) 256.
[20] T.W. Panunto, Z. Urbanczyk-Lipkowska, R.B. Johnson, M.C. Etter, J. Am. Chem. Soc. 109 (1987) 7786.
[21] J. Bernstein, M.C. Etter, J.M. MacDonald, J. Chem. Soc. Perkin Trans. II (1990) 695.
[22] J. Bernstein, R.E. Davis, L. Shimoni, N.-L. Chang, Angew. Chem. Int. Ed. Engl. 34 (1995) 1555.
[23] J. Grell, J. Bernstein, G. Tinhofer, Acta Cryst. B 55 (1999) 1030 (and references therein).
[24] A.T. Baker, P. Singh, V. Vignevich, Aust. J. Chem. 44 (1991) 1041.
[25] T. Steiner, J. Phys. Chem. 102 (1998) 7041.
[26] R. Taylor, O. Kennard, W.J. Versichel, J. Am. Chem. Soc. 106 (1984) 244.
[27] R. Taylor, O. Kennard, W.J. Versichel, J. Am. Chem. Soc. 105 (1983) 5761.
[28] H. Gunther, NMR Spectroscopy, 2, Wiley, New York, 1992.